# Incremental harmonic balance method for nonlinear flutter of an airfoil with uncertain-but-bounded parameters

**ARTICLE** *in* APPLIED MATHEMATICAL MODELLING · FEBRUARY 2012

Impact Factor: 2.25 · DOI: 10.1016/j.apm.2011.07.016



**3 AUTHORS:**

Y. M. Chen

**35** PUBLICATIONS **251** CITATIONS

SEE PROFILE

J.K. Liu

Sun Yat-Sen University

**148** PUBLICATIONS **757** CITATIONS

SEE PROFILE

Guang Meng

Shanghai Jiao Tong University

**516** PUBLICATIONS **3,314** CITATIONS

SEE PROFILE

Applied Mathematical Modelling 36 (2012) 657–667

Contents lists available at ScienceDirect

Applied Mathematical Modelling

journal homepage: www.elsevier.com/locate/apm

# Incremental harmonic balance method for nonlinear flutter of an airfoil with uncertain-but-bounded parameters

Y.M. Chen [a,*], J.K. Liu [a], G. Meng [b]

[a] Department of Mechanics, Sun Yat-sen University, 135 Xingangxi Road, Guangzhou 510275, China
[b] State Key Laboratory of Mechanical System and Vibration, Shanghai Jiao Tong University, 800 Dongchuan Road, Shanghai 200240, China

ARTICLE INFO

*Article history:*
Received 6 January 2010
Received in revised form 31 May 2011
Accepted 1 July 2011
Available online 12 July 2011

*Keywords:*
Nonlinear flutter
Limit cycle oscillation
Incremental harmonic balance method
Uncertainty
Statistic

ABSTRACT

The limit cycle oscillation of a two-dimensional airfoil with parameter variability in an incompressible flow is investigated using the incremental harmonic balance (IHB) method. The variable parameters, such as the wind speed, the cubic plunge and pitch stiffness coefficients, are modeled as either bounded uncertain or stochastic parameters. In the solution process of the IHB method, the bounded parameters are considered as an active increment. Taking all values over the considered bounded regions of the active parameters provides us with a series of IHB solutions of limit cycle oscillations of the airfoil. With the aid of the attained solutions, the bounds and some statistical properties of the limit cycle oscillations are determined and compared with Monte Carlo simulation (MCS) results. Numerical examples show that the proposed approach is valid and effective for analyzing strongly nonlinear vibration problems with bounded uncertainties.



## 1. Introduction

Airfoil flutter is one of the typical self-excited systems [1]. By extracting energy from the air, the airfoil can continue vibrating stably or unstably. Since 1950s, nonlinear flutter analysis has stimulated the interests and curiosity of many researchers [2]. As the flow velocity increases beyond the linear flutter speed, the motion oscillates with a limited amplitude, i.e., limit cycle oscillation. Predicting amplitude and frequency of flutter oscillations via analytical or numerical techniques has been an active area of research for many years [3–11].

As for qualified engineering systems, due to the tolerance design and/or other factors, uncertainties in these systems are usually inevitable [12]. Incorporating them into the flutter analysis becomes a commonly confronted yet cumbersome problem. Recent years have witnessed the applications and techniques related to the stochastic analysis of limit cycle oscillation (LCO). Attar and Dowell [13] employed the Monte Carlo simulation and a response surface method to map the output characteristics of a delta wing to two input parameters considered variable: thickness and modulus of elasticity. Similarly, Millman et al. [14] also gave special attention in the response surface mapping to the modeling of the bifurcation leading to LCO. Another technique, called stochastic Galerkin methods, was proposed by Xiu et al. [15] to capture LCOs arising in nonlinear systems with uncertainties. Pettit and Beran proposed one kind of method to study LCOs by using polynomial chaos [16] and Wiener–Haar expansion [17], respectively. Additionally, Millman et al. [18] applied Fourier chaos expansion to investigate the bifurcation behavior of an airfoil. The Gegenbauer polynomial can also be applied in the orthogonal decomposition of a stochastic nonlinear flutter system, as suggested by Wu et al. [19]. Basically, those expansion type techniques for nonlinear stochastic vibration method aim at transforming a stochastic problem into a deterministic one through special

* Corresponding author.
*E-mail address:* chenyanmao@hotmail.com (Y.M. Chen).

0307-904X/$ - see front matter © 2011 Elsevier Inc. All rights reserved.
doi:10.1016/j.apm.2011.07.016

representations of the output variables and/or stochastic processes. The *B*-spline stochastic projection technique was utilized to quantify uncertainty [20]. It was also extended, by Beran et al. [21], to the treatment of aerodynamic nonlinearities, as modeled through the discrete Euler equations.

As for structural vibration problems, while the literature is relatively rich in the stochastic analysis of problems that are either static, linear, or both [22–26], there is much less work directed towards describing nonlinear variables and processes that are dynamic with compact stochastic representations and with nonlinearities, especially strong ones. Nonetheless, recent years has witnessed some valuable researches on nonlinear systems with uncertainties. For instance, Worden et al. [27] studied the uncertainty propagation through a simple nonlinear system; Witteveen et al. [28] proposed a probabilistic collocation method to compute the limit cycle oscillations of a harmonic oscillator. In addition, the Monte Carlo simulation technique [29] and the non-probabilistic interval analysis method [30] were used to investigate nonlinear structural systems, respectively. A major reason consists in the fact that it is not easy to analyze nonlinear systems themselves. When uncertainties are taken into account, problems can become much tougher. To the best of our knowledge, only a little attention has been paid to investigating the effects of random parameters on the flutter, LCOs and peak responses of an airfoil, as mentioned above.

This paper presents a direct simulating approach based on the incremental harmonic balance method [31–33] to capture the bounds and/or statistical characteristics of an airfoil subject to either bounded non-probability uncertainties or stochastic parameters. While the considered uncertain variable changing over its given bounded region, it is considered as an active increment and incorporated in the solution procedures of the IHB method. For the cases that variables are given as non-probability, as long as the increment is chosen small enough, the bounds of LCOs can be accurately determined. While variables are stochastic, important and interesting statistical properties such as mean value, standard deviation and distribution function are obtained to excellent accuracy.

## 2. Equations of motion

The physical model given in Fig. 1 is a two-dimensional airfoil, oscillating in pitch and plunge, which has been employed by many authors. The pitch angle about the elastic axis is denoted by $\alpha$, positive with the nose up; the plunge deflection is denoted by $\bar{h}$, positive in the downward direction. The elastic axis is located at a distance $a_h b$ from the mid-chord, while the mass center is located at a distance $x_\alpha b$ from the elastic axis. Both distances are positive when measured towards the trailing edge of the airfoil. Let $r_\alpha b$ be the radius of gyration of the airfoil with respect to the elastic axis, $\omega_\xi$ and $\omega_\alpha$ be the eigenfrequencies of the constrained one-degree-of-freedom system associated with the linear plunging and the pitching springs, respectively. $c_\alpha$ and $c_\xi$ are the coefficients of damping in pitch and plunge, respectively.

In terms of non-dimensional time $t = \omega_\alpha t_1 (t_1$ is the real time) and non-dimensional plunge displacement $\xi = \bar{h}/b$, the coupled motions of the airfoil in incompressible steady flow can be described as [9]

$$\begin{cases} \mu\ddot{\xi} + \mu x_\alpha \ddot{\alpha} + \frac{c_\xi}{\pi\rho b^2 \omega_\alpha}\dot{\xi} + \mu\left(\frac{\omega_\xi}{\omega_\alpha}\right)^2 \frac{\partial V}{\partial \xi} = -2\left(\frac{u}{b\omega_\alpha}\right)^2 \alpha, \\ \mu x_\alpha \ddot{\xi} + \mu r_\alpha^2 \ddot{\alpha} + \frac{c_\alpha}{\pi\rho b^2 \omega_\alpha}\dot{\alpha} + \mu r_\alpha^2 \alpha \frac{\partial V}{\partial \alpha} = (1 + 2a_h)\left(\frac{u}{b\omega_\alpha}\right)^2 \alpha, \end{cases} \tag{1}$$

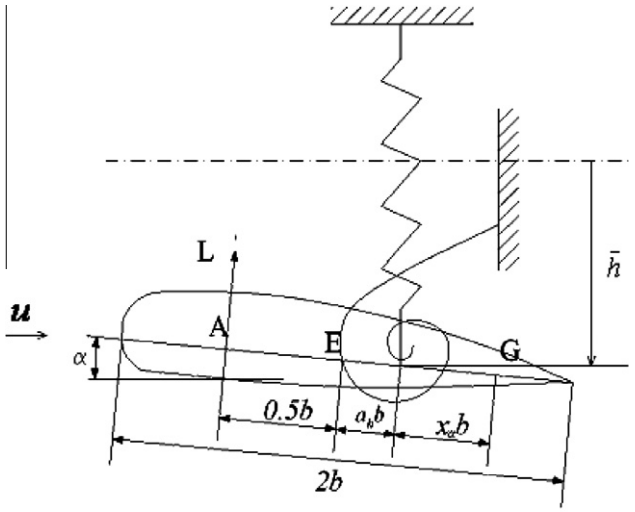


**Fig. 1.** Sketch of a two-dimensional airfoil.

where the superscript denotes the differentiation with respect to $t$. The symbol $V$ above represents the potential for the elastic restoring forces and in this study is given by

$$V = \frac{1}{2}\xi^2 + \frac{1}{2}\alpha^2 + \frac{1}{4}k_\xi\xi^4 + \frac{1}{4}k_\alpha\alpha^4, \tag{2}$$

where $k_\xi$ and $k_\alpha$ are bounded uncertain or stochastic parameters. Thus, we consider both the plunge and the pitch spring with cubic nonlinearities. Employing the values of the parameters adopted by Liu and Zhao [4]: $\mu = 20, a_h = -0.1, b = 1m, x_\alpha = 0.25, r_\alpha^2 = 0.5, \left(\frac{\omega_\xi}{\omega_\alpha}\right)^2 = 0.2, \omega_\alpha = 62.8$ Hz and the damping terms $0.1\dot{\xi}, 0.1\dot{\alpha}$, then Eq. (1) is rewritten as

$$\begin{aligned} &0.5\ddot{\xi} + 0.25\ddot{\alpha} + 0.1\dot{\xi} + 0.2\xi + 0.1Q\alpha + k_\xi\xi^3 = 0,\\ &0.25\ddot{\xi} + 0.5\ddot{\alpha} + 0.1\dot{\alpha} + (0.5 - 0.04Q)\alpha + k_\alpha\alpha^3 = 0, \end{aligned} \tag{3}$$

where $Q = \left(\frac{u}{b\omega_\alpha}\right)^2$ is called the generalized wind speed. For brevity, we denote $\mathbf{x} = [\xi, \alpha]^{\mathrm{T}}$ (the superscript "T" denotes the transpose), and rewrite Eq. (3) in vector form

$$\mathbf{M}\ddot{\mathbf{x}} + \boldsymbol{\mu}\dot{\mathbf{x}} + (\mathbf{K}_1 + \mathbf{K}_2 Q)\mathbf{x} + \mathbf{K}_3[\xi^3, \alpha^3]^{\mathrm{T}} = \mathbf{0}, \tag{4}$$

where

$$\mathbf{M} = \begin{bmatrix} 1 & 0.25 \\ 0.25 & 0.5 \end{bmatrix}, \quad \boldsymbol{\mu} = \begin{bmatrix} 0.1 & 0 \\ 0 & 0.1 \end{bmatrix}, \quad \mathbf{K}_1 = \begin{bmatrix} 0.2 & 0 \\ 0 & 0.5 \end{bmatrix}, \quad \mathbf{K}_2 = \begin{bmatrix} 0 & 0.1 \\ 0 & -0.04 \end{bmatrix},$$

and $\mathbf{K}_3 = \begin{bmatrix} k_\xi & 0 \\ 0 & k_\alpha \end{bmatrix}$. In Eq. (4), $Q$, $k_\xi$ and $k_\alpha$ are considered as either bounded uncertain or random parameters, which are given as

$$Q = Q_0 + Q_1 v, \quad k_\xi = k_{\xi 0} + k_{\xi 1} v, \quad k_\alpha = k_{\alpha 0} + k_{\alpha 1} v, \tag{5}$$

where $Q_0$, $k_{\xi 0}$ and $k_{\alpha 0}$ are the mean values and $Q_1$, $k_{\xi 1}$ and $k_{\alpha 1}$ are the double standard deviation of $Q$, $k_\xi$ and $k_\alpha$, respectively; $v \in [-1, 1]$ is given as a bounded uncertainty defined on $[-1, 1]$, or as a stochastic parameter with zero mean and a probability function $f(v)$, $-1 \leqslant v \leqslant 1$. This study deals with cases when only one uncertain parameter is involved in the above system, i.e., one of $Q$, $k_\xi$ and $k_\alpha$ is supposed to be uncertain or stochastic, which means only one of $Q_1$, $k_{\xi 1}$ and $k_{\alpha 1}$ is unequal to zero.

## 3. Incremental harmonic balance method

First of all, introduce a new time scale $\tau = \omega t$, where $\omega$ is the angular frequency of the limit cycle oscillation, then Eq. (4) becomes

$$\omega^2\mathbf{M}\mathbf{x}'' + \omega\boldsymbol{\mu}\mathbf{x}' + (\mathbf{K}_1 + \mathbf{K}_2 Q)\mathbf{x} + \mathbf{K}_3[\xi^3, \alpha^3]^{\mathrm{T}} = \mathbf{0}. \tag{6}$$

The first step of the IHB method is a Newton–Raphson procedure. Let $\mathbf{x}_i$ and $\omega_i$ denote a state of vibration corresponding to $v = v_i$, the neighboring state can be expressed by adding the corresponding increments to them as follows

$$\mathbf{x} = \mathbf{x}_i + \Delta\mathbf{x}, \quad \omega = \omega_i + \Delta\omega, \quad v = v_i + \Delta v. \tag{7}$$

Substituting Eq. (7) into (6) and neglecting all small terms of higher order, one obtains the following linearized incremental equation

$$\omega_i^2\mathbf{M}\Delta\mathbf{x}'' + \omega_i\boldsymbol{\mu}\Delta\mathbf{x}' + \mathbf{K}_\mathbf{x}\Delta\mathbf{x} + \mathbf{K}_\omega\Delta\omega + \mathbf{K}_v\Delta v + \mathbf{R}(\mathbf{x}_i, \omega_i, v_i) = 0, \tag{8}$$

where

$$\mathbf{K}_\mathbf{x} = \mathbf{K}_1 + \mathbf{K}_2(Q_0 + Q_1 v_i) + 3\mathbf{K}_{3,i}\left[\xi_i^2, \alpha_i^2\right]^{\mathrm{T}}, \quad \mathbf{K}_{3,i} = \begin{bmatrix} (k_{\xi 0} + k_{\xi 1} v_i)^2 & 0 \\ 0 & (k_{\alpha 0} + k_{\alpha 1} v_i)^2 \end{bmatrix},$$

$$\mathbf{K}_\omega = 2\omega_i\mathbf{M}\mathbf{x}_i'' + \boldsymbol{\mu}\mathbf{x}_i', \quad \mathbf{K}_v = \mathbf{K}_2 Q_1 \mathbf{x}_i + \begin{bmatrix} k_{\xi 1} & 0 \\ 0 & k_{\alpha 1} \end{bmatrix}[\xi_1^3, \alpha_1^3]^{\mathrm{T}}$$

and the residual

$$\mathbf{R}(\mathbf{x}_i, \omega_i, v_i) = \omega_i^2\mathbf{M}\mathbf{x}_i'' + \omega_i\boldsymbol{\mu}\mathbf{x}_i' + (\mathbf{K}_1 + \mathbf{K}_2 Q_0 + \mathbf{K}_2 Q_1 v_i)\mathbf{x}_i + \begin{bmatrix} k_{\xi 0} + k_{\xi 1} v_i & 0 \\ 0 & k_{\alpha 0} + k_{\alpha 1} v_i \end{bmatrix}\begin{bmatrix} \xi_i^3 \\ \alpha_i^3 \end{bmatrix}$$

goes to zero as $x_i$ and $\omega_i$ approach the exact solutions.

The second step is the Ritz–Garlerkin procedure, let

$$\mathbf{x}_i = \frac{1}{2}\mathbf{a}_0 + \sum_{n=1}^{N}[\mathbf{a}_n \cos(n\tau) + \mathbf{b}_n \sin(n\tau)], \tag{9}$$

$$\Delta\mathbf{x} = \frac{1}{2}\Delta\mathbf{a}_0 + \sum_{n=1}^{N}[\Delta\mathbf{a}_n \cos(n\tau) + \Delta\mathbf{b}_n \sin(n\tau)]. \tag{10}$$

Substituting Eqs. (9) and (10) into (8), and implementing the Garlerkin procedure, one can obtain a set of linear equations in terms of

$$\mathbf{K}_\mathbf{u}\Delta\mathbf{u} + \mathbf{K}_\omega\Delta\omega + \mathbf{K}_v\Delta v + \mathbf{K}_R = 0, \tag{11}$$

where $\Delta\mathbf{u} = [\Delta a_{01}, \Delta a_{02}, \Delta a_{11}, \Delta a_{12}, \Delta b_{11}, \Delta b_{12}, \ldots, \Delta b_{N1}, \Delta b_{N2}]^{\mathrm{T}}$, $\mathbf{K}_\mathbf{u}$ is the Jacobian square matrix of dimension $2(2N+1)$; $\mathbf{K}_\omega$ is the frequency gradient vector; $\mathbf{K}_v$ is the parametric gradient vector; and $\mathbf{K}_R$ is the residue vector. These matrixes and vectors depend upon the initial solutions $\mathbf{x}_i$, $\omega_i$ and $v_i$. In the IHB method, usually, one parameter varying actively (called as the active increment) should be chosen to control the continuations of solutions. Here, $v$ is taken as the active incrementing parameter, thus $\Delta v$ can be given as a very small quantity. Note that Eq. (11) contains $2(2N+1)$ equations while $2(2N+1)+1$ unknowns. Therefore, the unknowns cannot be determined directly through solving this equation. One of the Fourier coefficients is fixed to be zero in the solution procedure, as adopted by many other applications of the IHB method. Then, Eq. (11) describes a set of equations in the increments $\Delta\mathbf{u}$ and $\Delta\omega$ at each step, which can be solved iteratively.

## 4. Path following

Along an equilibrium path for varying $v$, it is possible that the solution curve may form a loop (when the Jacobian matrix $\mathbf{K}_u$ is singular). In order to eliminate the singular behavior of $\mathbf{K}_u$, one may use either the selective coefficient or the arc-length method [34]. The latter method is utilized here.

Introducing the path parameter $\eta$, one has the augmenting equation

$$g(\mathbf{u}, \omega, v) - \eta = 0, \quad \text{or} \quad g(\mathbf{w}) - \eta = 0. \tag{12}$$

The function $g = \mathbf{w}^{\mathrm{T}}\mathbf{w}$ is a good choice. Taking increments on $\mathbf{w}$ and $\eta$ in Eq. (12), one has

$$\frac{\partial g}{\partial \mathbf{u}^{\mathrm{T}}}\Delta\mathbf{u} + \frac{\partial g}{\partial \omega}\Delta\omega + \frac{\partial g}{\partial v}\Delta v - \Delta\eta + g - \eta = 0. \tag{13}$$

Together with Eq. (11), one has the augmented incremental equation

$$\mathbf{K}_w\Delta\mathbf{w} = \begin{bmatrix} \mathbf{K}_u & \mathbf{K}_\omega & \mathbf{K}_v \\ (\partial g/\partial \mathbf{u})^{\mathrm{T}} & \partial g/\partial\omega & \partial g/\partial v \end{bmatrix}\Delta\mathbf{w} = -\begin{bmatrix} \mathbf{K}_R \\ g - \eta \end{bmatrix}, \tag{14}$$

where $\mathbf{K}_w$ is the Jacobian (tangential) matrix with respect to $\mathbf{w}$. The arc-length parameter $\eta$ can be taken as the control parameter in constructing the solution curve with respect to $v$.

## 5. Mathematical formulation

In this section, we will apply the incremental harmonic balance method proposed above to directly simulate the LCOs of the flutter system with bounded uncertain or random parameters. Here, the bounds and stochastic properties of the LCOs are determined. For brevity, denote $H$ and $A$ as the amplitudes the LCOs in the plunge and pitch DOFs respectively. In essence, the amplitudes and frequency can be considered as functions of varying parameter $v$, i.e., $A(v)$, $H(v)$ and $\omega(v)$, respectively. Letting $v_0 = -1$, and applying the iteration scheme (14) repeatedly until $v$ approaches $v_N = 1$, then one obtains a series of approximations for $H(v_i)$, $A(v_i)$ and $\omega(v_i)$, corresponding to $v = v_i$.

*Case 1*: Eq. (4) contains one bounded uncertain parameter (non-probability). For this case, one would probably care about the extreme responses of the airfoil, i.e., the maximum and/or minimum values of the amplitudes and frequencies of the LCOs. As long as the increment of the length of the solution curve, i.e., $\Delta\eta$ is given small enough, one can obtain the extremes of $H$, $A$ and $\omega$ just by comparing the values of $H(v_i)$, $A(v_i)$ and $\omega(v_i)$. For example, the maximum and minimum values of $A$ can be given as $\max\{A(v_i), i = 0, 1, 2, \ldots, N\}$ and $\min\{A(v_i), i = 0, 1, 2, \ldots, N\}$, respectively.

*Case 2*: Eq. (4) contains one bounded stochastic parameter. The LCOs are crucial for the safely handling and life estimations of aircraft. It is, therefore, fundamentally interesting and necessary to investigate the mean values, the standard deviations and the distribution functions of $H$, $A$ and $\omega$. In essence, the amplitudes and frequency of the LCOs can be investigated as random functions of stochastic parameter $v$. Take $A$ as an illustrative example to propose the procedures for obtaining the statistical properties of the LCOs. Mathematically, the mean value and standard deviation of $A$ can be given, respectively, as follows

$$E_v A = \int_{-1}^{1} A(v) f(v) dv, \tag{15}$$

$$D_v A = \sqrt{\int_{-1}^{1} A^2(v) f(v) dv - (E_v A)^2}. \tag{16}$$

In the above algorithm, variable $v$ changes step by step with a tunable step length. Assume a series of limit cycle solutions are obtained corresponding to points $v = v_i$, $i = 0, 1, 2, \ldots, N$, with the amplitude in pitch as $A(v_i)$. Then, as long as $v$ varies very slowly, Eqs. (15) and (16) can be respectively approximated using the following cumulative sums

$$E_v A \approx \sum_{i=0}^{N-1} A(v_i) f(v_i) \Delta v = \sum_{i=0}^{N-1} A(v_i) f(v_i) |v_{i+1} - v_i|, \tag{17}$$

$$D_v A \approx \sqrt{\sum_{i=0}^{N-1} A^2(v_i) f(v_i) |v_{i+1} - v_i| - (E_v A)^2}. \tag{18}$$

Denote the distribution function of $A(v)$ as $F_A(a)$, one knows that

$$F_A(a) = \text{probability}\{A(v) \leqslant a\} = \int_{\Omega(a)} f(v) dv, \tag{19}$$

where the domain of integration $\Omega(a) = \{v | A(v) \leqslant a, -1 \leqslant v \leqslant 1\}$. First, we re-arrange the series $\{A(v_i), i = 0, 1, 2, \ldots, N\}$ from the minimum to maximum, that is,

$$\left\{ A(v_{m_j}),\ j = 0, 1, 2, \ldots, N,\ m_j \in \{0, 1, 2, \ldots, N\},\ A(v_{m_0}) \leqslant A(v_{m_1}) \leqslant \cdots \leqslant A(v_{m_N}) \right\}. \tag{20}$$

For any given $a$ except that $a \leqslant A(v_{m_0})$ or $a > A(v_{m_N})$, there exists one $J$ that $A(v_{m_J}) < a \leqslant A(v_{m_{J+1}})$ is true. In order to obtain the approximation of $F_A(a)$ using discrete values of $f(v_{m_j}), j = 0, 1, 2, \ldots, J, \Omega(a)$ can be approximately given as a discrete set $\{A(v_{m_j}) | j = 0, 1, 2, \ldots, J+1\} \subset \Omega(a)$. Then, Eq. (19) can be approximately obtained as

$$F_A(a) = \sum_{j=0}^{J+1} f(v_{m_j}) |v_{m_{j+1}} - v_{m_j}|. \tag{21}$$

One can see that as long as step length is chosen small enough, as, $F_A(a)$ approaches 0 and 1 when $J$ approaches 1 and $N - 1$, respectively. This can partly show the validity of Eq. (21).

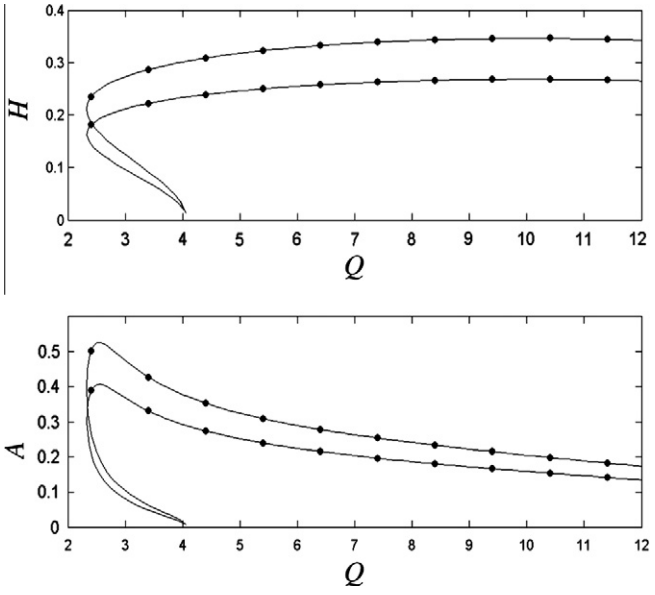


**Fig. 2.** Bounds of the amplitudes of the LCOs for Example I, where the heavy dots denote the MCS results.

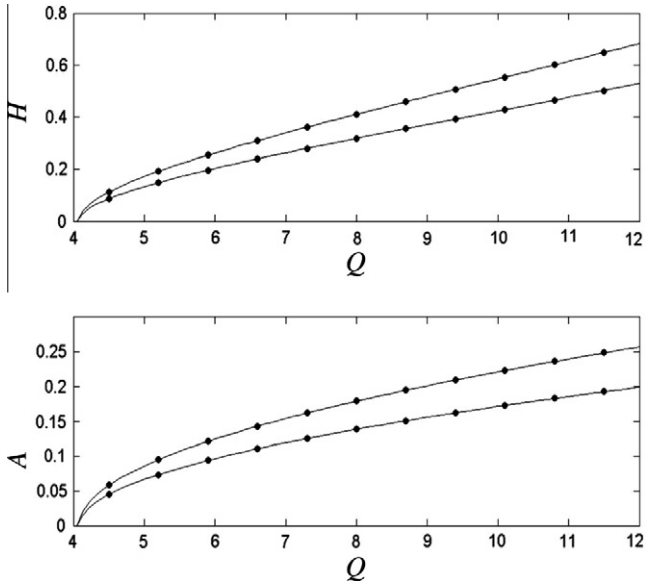


**Fig. 3.** Bounds of the amplitudes of the LCOs for Example II, where the heavy dots denote the MCS results.

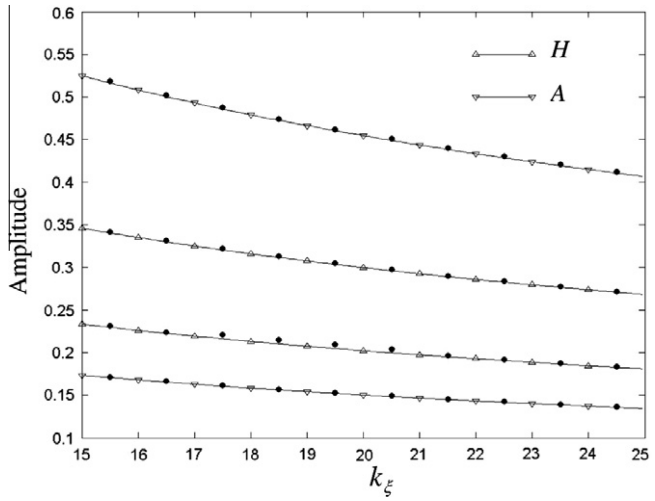


**Fig. 4.** Bounds of the amplitudes of LCOs, where the heavy dots denote MCS results.

## 6. Numerical examples

*Case 1: Non-probable Parameter*

If the coefficient of cubic plunging or pitching stiffness is uncertain, for Example I: $k_\xi = 20$, $k_{\xi 1} = 5$ and; or Example II: $k_\alpha = 20$, $k_{\alpha 1} = 5$ and $Q_1 = k_\xi = k_{\xi 1} = 0$, implementing the procedures proposed above, we obtain the extreme values of the amplitudes of the LCOs, as shown in Figs. 2 and 3. Because the frequency of the LCOs of the airfoil is independent of the coefficients of the cubic plunging and the pitching stiffness [9], the frequency is not considered here. As one can see, the numerical results attained by the proposed approach are in excellent agreement with the MCS results with 800 samples. In the MCS, the fourth-order Ronge–Kutta integrating method are used to capture the LCOs. There is a subcritical (supercritical) Hopf bifurcation point for Example I and II, respectively. Note that, the posterior limit cycle arising before the subcritical Hopf bifurcation point is unstable. Notice also that, numerical RK time-marching method is incapable of capturing unstable limit cycle solution [7]. Therefore, the unstable limit cycle solutions (in Fig. 2) cannot be validated by MCS results. In addition, as the amplitudes increase the discrepancies between the maximum and the minimum enlarge. As for Example II, the amplitudes increase

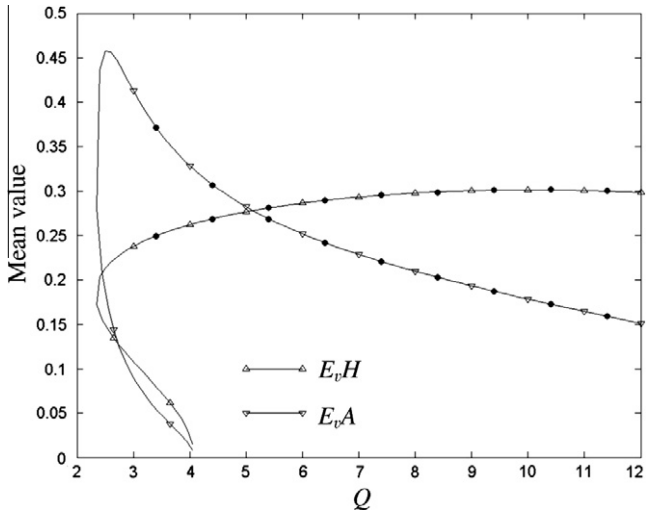


**Fig. 5.** Mean values of the amplitudes of the LCOs, where the heavy dots represent the MCS results, $k_{\xi 0} = 20$, $k_{\xi 1} = 5$ and $Q_1 = k_{\alpha 0} = k_{\alpha 1} = 0$.

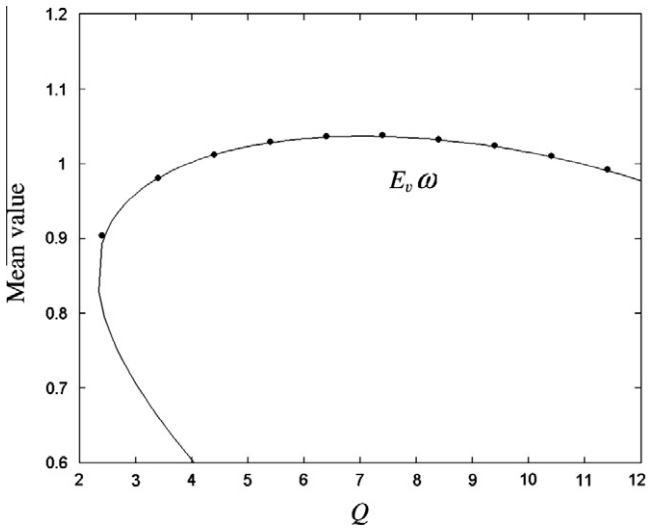


**Fig. 6.** Mean values of the frequency of the LCOs, where the heavy dots represent the MCS results, $k_{\xi 0} = 20$, $k_{\xi 1} = 5$ and $Q_1 = k_{\alpha 0} = k_{\alpha 1} = 0$.

monotonically with the wind speed $Q$, while for Example I they vary versus $Q$ much more complicatedly. First, both $H$ and $A$ increase rapidly once after the subcritical bifurcation occurs, but $A$ takes its maximum before does $H$. After that, they both decrease monotonically as the wind speed increases, respectively.

In both the above examples, the amplitudes of the LCOs reach their maximum values when the coefficient of cubic nonlinear stiffness approaches its lower bound, and vice versa. It is effective yet seems to be unnecessary to use the above stated method to predict the bounds of the LCOs, because for these simple cases one need only study the bounds of the considered parameters. As the wind speed varies, however, the extreme limit cycle behaviors reach their bounds in a much more complex manner (as shown in Fig. 2). For example, while considering the case that the wind speed varies in a bounded region, i.e., $Q_0 = 2.85$, $Q_1 = 0.5$, $k_{\xi 0} = 20$ and $k_{\xi 1} = k_{\alpha} = k_{\alpha 1} = 0$, we apply the proposed algorithm and obtain the extreme values of the amplitudes of the LCOs, as shown in Fig. 4. In this complicated example, the proposed approach is still very valid and effective.

*Case 2: Stochastic parameter*

As for the case when the flutter system contains one random parameter, the mean values, the standard deviations and the distribution functions of the amplitudes of the LCOs can be determined by using Eqs. (17), (18) and (21), respectively. A bounded probability density function with mono-peak and symmetrically distributed within $[-1,1]$, named as arc-like probability density function can be defined as follows [12]

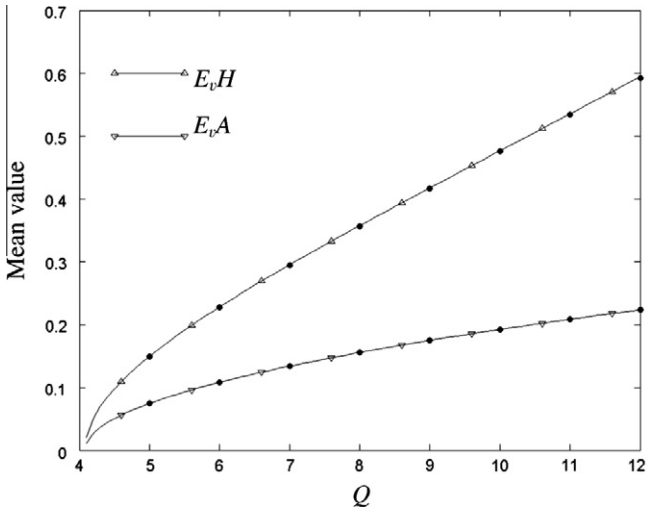


**Fig. 7.** Mean values of the amplitudes of the LCOs, where the heavy dots represent the MCS results, $k_{\alpha 0} = 20$, $k_{\alpha 1} = 5$ and $Q_1 = k_{\xi 0} = k_{\xi 1} = 0$.

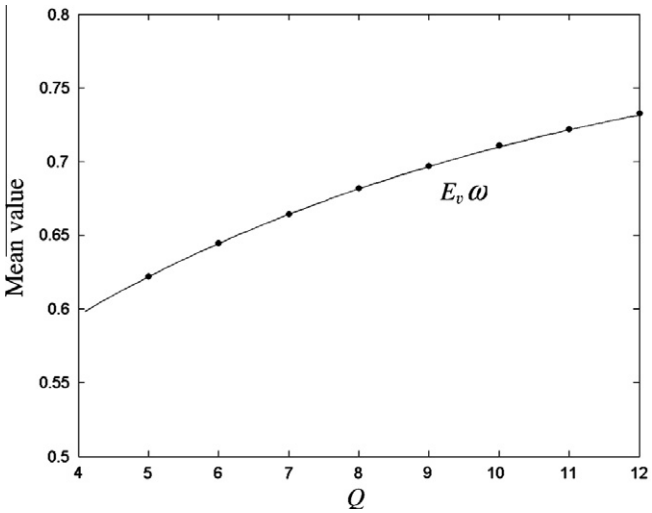


**Fig. 8.** Mean value of the frequency of the LCOs, where the heavy dots represent the MCS results, $k_{\alpha 0} = 20$, $k_{\alpha 1} = 5$ and $Q_1 = k_{\xi 0} = k_{\xi 1} = 0$.

$$f(v) = \begin{cases} \frac{2}{\pi}\sqrt{1-v^2} & |v| \leqslant 1, \\ 0 & |v| > 1. \end{cases} \tag{22}$$

In the following parts, it is taken as an illustration to test the proposed approach.

Figs. 5–8 show the comparisons between the mean values the amplitudes and frequency of the LCOs attained by the proposed approach and those computed by MCS. Note that, in the solution procedure of the presented method, the increment of the arc-length of the solution curve is chosen as $\Delta\eta = 0.01$. Corresponding to this incrementing quantity, the increment of the stochastic variable $v$ (i.e., $\Delta v$) is less than yet approximately equals to 0.01. Thus, without big loops in the solution curve, there are about 200 IHB results, i.e., $N \approx 200$. From those figures, excellent agreement can be easily observed. Similarly, the unstable limit cycle solutions cannot be directly computed by RK method, so that parts of the solutions have not been verified by MCS results, as shown in Fig. 5. Nonetheless, high accuracy of most solutions validated by MCS results still shows that the proposed approach is effective.

It is worth pointing out that the considered problems are strongly nonlinear ones. Furthermore, as Figs. 5–8 show, no matter how large the amplitudes are, the attained results take high accuracy. Thus, the proposed approach can be applicable to highly nonlinear vibration problems, no matter whether or not large-amplitude vibration arises.

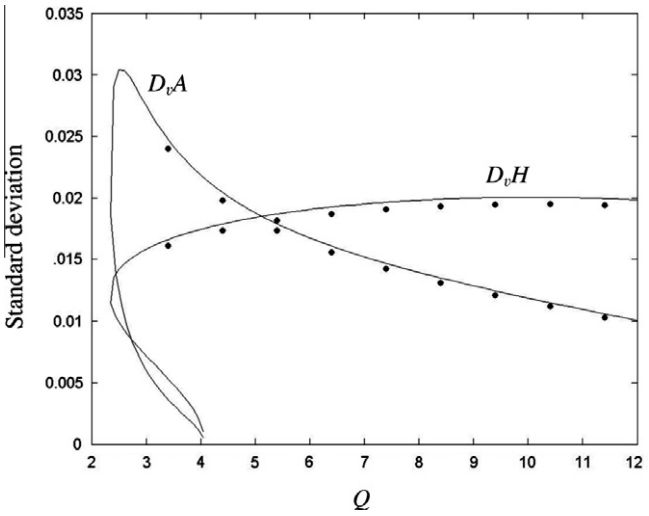


**Fig. 9.** Standard deviations of the amplitudes of the LCOs, where the heavy dots represent the MCS results, $k_{\xi 0} = 20$, $k_{\xi 1} = 5$ and $Q_1 = k_{\alpha 0} = k_{\alpha 1} = 0$.

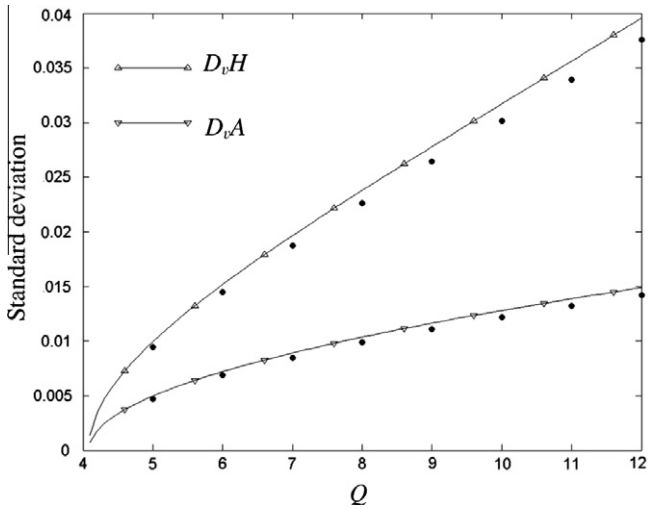


**Fig. 10.** Standard deviations of the amplitudes of the LCOs, where the heavy dots represent the MCS results, $k_{\alpha 0} = 20$, $k_{\alpha 1} = 5$ and $Q_1 = k_{\xi 0} = k_{\xi 1} = 0$.

The standard deviations of the amplitudes of the LCOs are plotted in Figs. 9 and 10, corresponding to the cases when the flutter system includes cubic plunging and pitching stiffness, respectively. The attained solutions are still in good excellent agreement with the MCS results. Because the frequency of the LCOs of flutter system (4) is independent of the coefficients of the cubic plunging and pitching stiffness as pointed out in Ref. [7], its standard deviation actually remains the same while $v$ varying. Therefore, the standard deviation of the frequency is not presented here. In addition, as one can see, the curves in Figs. 9 and 10 are rather similar to those of the corresponding mean values, which implies that the standard deviations are roughly proportional to the mean values. Taking Figs. 5 and 9 for example, as the wind speed is chosen as $Q = 12$, we have $D_vH/E_v H \approx 6\%$, and the relative error of the results attained by the presented method is less than 5%. Thus, from both theoretical and engineering viewpoints, the proposed approach is utilizable.

The distribution functions of the amplitudes of the LCOs are shown in Figs. 11 and 12, denoting the cases when either random cubic plunging stiffness or random wind speed is included in the analysis. The numerical solutions provided by the presented method are almost the same as the MCS results with 800 samples. The proposed approach is indeed capable of constructing the distribution functions of the limit cycle behaviors. As is stated above, the frequency of the LCOs is independent of $k_\xi$ and varies very slowly with respect to $Q$, so that the frequency remains the same or changes a little at most when $v$ varying. Therefore, it is not equally important and interesting to investigate the distribution of the frequency.

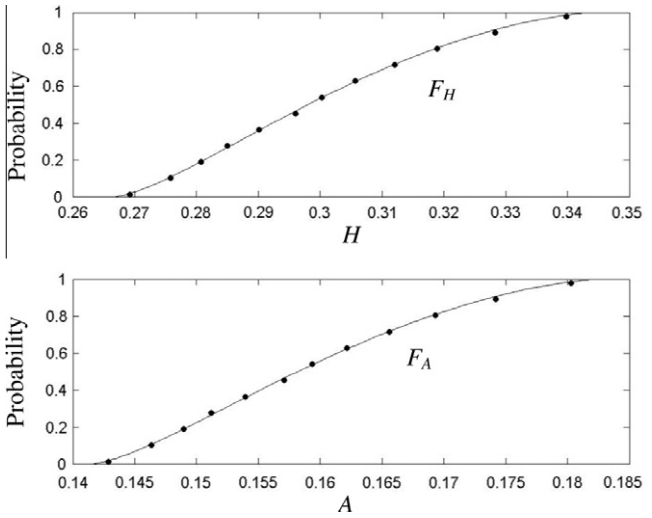


**Fig. 11.** Distribution functions of the amplitudes of the LCOs, where the heavy dots represent the MCS results, $k_{\xi 0} = 20$, $k_{\xi 1} = 5$, $Q_0 = 11.4$ and $Q_1 = k_{\alpha 0} = k_{\alpha 1} = 0$.

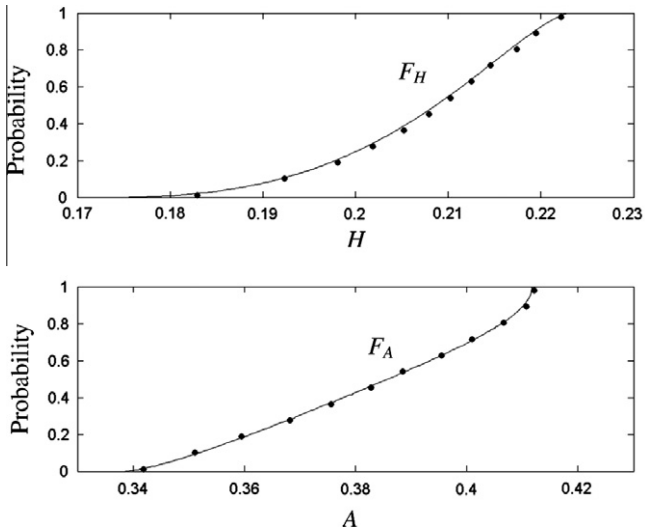


**Fig. 12.** Distribution functions of the amplitudes of the LCOs, where the heavy dots represent the MCS results, $k_{\xi 0} = 24.5$, $Q_0 = 2.85$, $Q_1 = 0.5$ and $k_{\xi 1} = k_{\alpha 0} = k_{\alpha 1} = 0$.

As one can see, there are large discrepancies between the distribution curves in Fig. 11 and those in Fig. 12. In the former, the slope for small amplitudes is relatively larger than that for large ones, while in the latter the contrary is true. According to Fig. 4, the slope of the curves of $H$ and $A$ versus $k_\xi$ decreases with $A$ decreasing (when $k_\xi$ increases). That implies, for the same decreasing quantities of $H$ and $A$, it needs larger and larger incrementing of $k_\xi$, i.e., $\Delta k_\xi$, as $k_\xi$ increases. In other words, if $k_\xi$ is uniformly distributed in a bounded region, $H$ and $A$ will have a larger probability of taking relatively small values. That is the reason why the slope of the distribution curves in Fig. 11 is relatively large at small amplitudes. In order to explain the contrary shown in Fig. 12, one should refer to Fig. 5. As it is shown, first the slope of $H$ curve is positive and becomes smaller and smaller as $Q$ increases. Therefore, in the case for the distribution curve of $H$ in Fig. 12 that, contrary to that for Fig. 11, it is more probable for the flutter system to give rise up LCOs with relatively large amplitudes$H$. Nevertheless, for the distribution curve of $A$ in Fig. 12, that why large values of $A$ arise more probably can not be explained by similar reason. In fact, it is more direct and simple. It is just because when $Q = Q_0 + 0.5v$ varies in $[2.35, 3.35]$, relatively large values of $A$ can possibly occur twice, as is shown in Fig. 5. In short, no matter how the distribution curves change, the presented approach in this paper can provide correct analysis results, which could be compatible with the real physical system.

## 7. Conclusions

Based on the IHB method, we have proposed an approach for capturing the limit cycle oscillations of an airfoil with strongly nonlinear cubic stiffness, which is subject to either non-probability but bounded uncertainty or bounded stochastic parameters. In the construction of IHB iterative algorithm, the considered variables are treated as active increments. After they take all values over the given bounded regions, a series of solutions for LCOs are obtained and then used to directly simulate the uncertain properties of limit cycle behaviors of the considered flutter system. The presented technique is tested through several numerical examples, including those having non-probability but bounded uncertainty and such containing randomness. Excellent agreement of the solutions given by the proposed method with MCS results are observed for both cases, which implies this approach would be applicable to more nonlinear, especially strongly ones, vibration problems subject to either non-probability or stochastic uncertainties.

## Acknowledgements

This work is supported by the NSFC (10102023, 10972241, 11002088 and 10732060), and Research Fund of State Key Lab of MSV, China (Grant No.MSV-MS-2010-9), and Project granted by granted by "985 project" of Sun Yat-sen University.

## References

[1] E.H. Dowell, R. Clark, D. Cox, et al, A Modern Course in Aeroelasticity, Kluwer Academic Publishers., Dordrecht, 2004.
[2] B.H.K. Lee, S.J. Price, Y.S. Wong, Nonlinear aeroelastic analysis of airfoils: bifurcation and chaos, Progress Aerosp. Sci. 35 (1999) 205–344.
[3] S.F. Price, H. Alighanbari, B.H.K. Lee, The aeroelastic response of a two-dimensional airfoil with bilinear and cubic structural nonlinearities, J. Fluids Struct. 9 (1995) 175–193.
[4] J.K. Liu, L.C. Zhao, Bifurcation analysis of airfoils in incompressible flow, J. Sound Vibr. 154 (1) (1992) 117–124.
[5] P. Shahrzad, M. Mahzoon, Limit cycle flutter of airfoils in steady and unsteady flows, J. Sound Vibr. 256 (2) (2002) 213–225.
[6] L.P. Liu, E.H. Dowell, Harmonic balance approach for an airfoil with a freeplay control surface, AIAA J. 43 (4) (2005) 802–815.
[7] L.P. Liu, E.H. Dowell, The secondary bifurcation of an aeroelastic airfoil motion: effect of high harmonics, Nonlinear Dyn. 37 (2004) 31–49.
[8] B.D. Coller, P.A. Chamara, Structural non-linearities and the nature of the classic flutter instability, J. Sound Vibr. 277 (2004) 711–739.
[9] Y.M. Chen, J.K. Liu, Homotopy analysis method for limit cycle flutter of airfoils, Appl. Math. Comput. 203 (2) (2008) 854–863.
[10] Y.M. Chen, J.K. Liu, On the limit cycles of aeroelastic systems with quadratic nonlinearities, Struct. Eng. Mech. 30 (1) (2008) 67–76.
[11] Y.M. Chen, J.K. Liu, Elliptic harmonic balance method for two degree-of-freedom self-excited oscillators, Commun. Nonlinear Sci. Numer. Simulat. 14 (2009) 916–922.
[12] T. Fang, X.L. Leng, C.Q. Song, Chebyshev polynomial approximation for dynamical response problems of random structures, J. Sound Vibr. 266 (2003) 198–206.
[13] P.J. Attar, E.H. Dowell, A stochastic analysis of the limit cycle behavior of a nonlinear aeroelastic model using the response surface method. in: AIAA 2005–1986, April, 2005.
[14] D.R. Millman, P.I. King, R.C. Maple, P.S. Beran, Predicting uncertainty propagation in a highly nonlinear system with a stochastic projection method, in: 45th AIAA/ASCE/AHS/ASC Structures, Structural Dynamics, and Materials Conference, AIAA 2004–1613, April, 2004.
[15] D. Xiu, I.G. Kevrekidis, R. Ghanem, An equation-free, multiscale approach to uncertainty quantification, Comput. Sci. Eng. 7 (3) (2005) 16–23.
[16] C.L. Pettit, P.S. Beran, Polynomial chaos expansion applied to airfoil limit cycle oscillations. in: AIAA 2004–1691, April, 2004.
[17] C.L. Pettit, P.S. Beran, Wiener–Haar expansion of airfoil limit cycle oscillations. in: AIAA 2005–1985, April, 2005.
[18] D.R. Millman, P.I. King, P.S. Beran, Airfoil pith-and-plunge bifurcation behavior with Fourier chaos expansion, J. Aircraft 42 (2005) 376–384.
[19] C.L. Wu, H.M. Zhang, T. Fang, Flutter analysis of an airfoil with bounded random parameters in incompressible flow via Gegenbauer polynomial approximation, Aerosp. Sci. Tech. 11 (2007) 518–526.
[20] D.R. Millman, P.I. King, R.C. Maple, P.S. Beran, L.K. Chilton, Uncertainty quantification with a *B*-spline stochastic projection, AIAA J. 44 (2006) 1845–1853.
[21] P.S. Beran, C.L. Pettit, D.R. Millman, Uncertainty quantification of limit-cycle oscillations, J. Comput. Phys. 217 (2006) 217–247.
[22] I. Elishakoff, Probabilistic Methods in the Theory of Structures, John Wiley & Sons, 1983.
[23] W.L. Oberkampf, S.M. Deland, B.M. Rutherford, K.V. Diegert, K.F. Alvin, Error and uncertainty in modeling and simulation, Reliab. Eng. Syst. Safety 75 (2002) 333–357.
[24] E. Capiez-Lernout, M. Pellissetti, H. Pradlwarter, G.I. Schueller, C. Soize, Data and model uncertainties in complex aerospace engineering systems, J. Sound Vibr. 295 (2006) 923–938.
[25] Z.P. Qiu, Z. Ni, An inequality model for solving interval dynamic response of structures with uncertain-but-bounded parameters, Appl. Math. Model. (2009), doi:10.1016/j.apm.2009.10.028.
[26] T. Schultz, M. Sheplak, L.N. Cattafesta, Application of multivariate uncertainty analysis to frequency response function estimates, J. Sound Vibr. 205 (2007) 116–133.
[27] K. Worden, G. Manson, T.M. Lord, M.I. Friswell, Some observations on uncertainty propagation through a simple nonlinear system, J. Sound Vibr. 288 (2005) 601–621.
[28] J.A.S. Witteveen, A. Loeven, S. Sarkar, H. Bijl, Probabilistic collocation for period-1 limit cycle oscillations, J. Sound Vibr. 311 (2008) 421–439.
[29] Z.P. Qiu, L.H. Ma, X.J. Wang, Non-probabilistic interval analysis method for dynamic response analysis of nonlinear systems with uncertainty, J. Sound Vibr. 319 (2009) 531–540.
[30] B.N. Singh, A.K.S. Bisht, M.K. Pandit, K.K. Shukla, Nonlinear free vibration analysis of composite plates with material uncertainties: a Monte Carlo simulation approach, J. Sound Vibr. 324 (2009) 126–138.
[31] S.L. Lau, Y.K. Cheung, Amplitude incremental variational principle for nonlinear vibration of elastic systems, ASME J. Appl. Mech. 48 (1981) 959–964.
[32] Y.K. Cheung, S.H. Chen, S.L. Lau, Application of the incremental harmonic balance method to cubic non-linearity systems, J. Sound Vibr. 140 (1990) 273–286.
[33] A. Raghothama, S. Narayanan, Non-linear dynamics of a two-dimensional airfoil by incremental harmonic balance method, J. Sound Vibr. 226 (1999) 493–517.
[34] R. Seydel, From Equilibrium to Chaos, Elesvier, New York, 1988.